Exploring Hydrogenation and Fluorination in Curved 2D Carbon Systems: A Density Functional Theory Study on Corannulene

4 AUTHORS, INCLUDING:

Renato Batista Santos
Universidade Federal da Bahia
7 PUBLICATIONS   40 CITATIONS

SEE PROFILE

Roberto Rivelino
Universidade Federal da Bahia
66 PUBLICATIONS   621 CITATIONS

SEE PROFILE

G.K. Gueorguiev
Linköping University
46 PUBLICATIONS   512 CITATIONS

SEE PROFILE

Exploring Hydrogenation and Fluorination in Curved 2D Carbon Systems: A Density Functional Theory Study on Corannulene

Renato B. dos Santos,*,[†] Roberto Rivelino,*,[†] Fernando de B. Mota,*,[†] and Gueorgui K. Gueorguiev*,[‡]

[†]Instituto de Física, Universidade Federal da Bahia, 40210-340 Salvador, Bahia, Brazil
[‡]Department of Physics, Chemistry, and Biology, IFM, Linköping University, SE-58183 Linköping, Sweden

S Supporting Information

ABSTRACT: Corannulene has been a useful prototype for studying C-based nanostructures as well as surface chemistry and reactivity of sp^2-hybridized carbon-based materials. We have investigated fluorination and hydrogenation of corannulene carrying out density functional theory calculations. In general, the fluorination is energetically more favorable than hydrogenation of corannulene. The substitution of the peripheral H atoms in the corannulene molecule by F atoms leads to a larger cohesive energy gain than when F (or H) atoms are bonded to the hub carbon and bridge carbon sites of this molecule. As expected for doped C-based nanostructures, the hydrogenation or fluorination significantly changes the HOMO−LUMO gap of the system. We have obtained HOMO−LUMO gap variations of 0.13−3.46 eV for F-doped and 0.38−1.52 eV for H-doped systems. These variations strongly depend on the concentration and position of the incorporated F/H atoms, instead of the structural stability of the doped systems. Considering these calculations, we avoid practical difficulties associated with the addition/substitution reactions of larger curved two-dimensional (2D) carbon nanostructures, and we obtain a comprehensive and systematic understanding of a variety of F/H 2D doped systems.
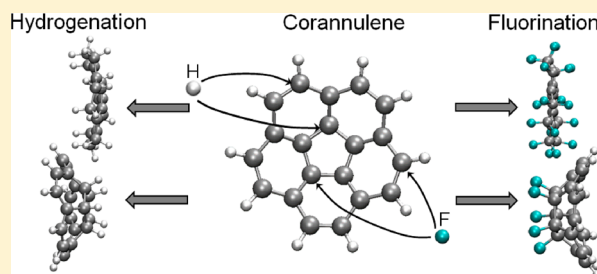
1. INTRODUCTION

Fluorination is one of the most effective chemical approaches for both modifying and controlling the properties of conventional C-based materials[1−4] as well as for functionalizing nanostructured C-based systems such as nanotubes[1,5] and graphene.[6−8] Studies on the fluorination of graphene have demonstrated that a fluorographene-like system is thermodynamically stable.[9] Also, such systems can exhibit a larger band gap[10] and higher mechanical strength, as compared to pure graphene, as well as to charged surfaces.[11] The reason for the efficiency of fluorine as modifying agent is due to its high chemical reactivity and to its extreme electronegativity (in fact, F is the most electronegative chemical element).

In an experimental study of multiwalled carbon nanotubes, Takuya et al.[5] have demonstrated that the fluorination can be used to suppress the optical properties of the outer carbon nanotubes without interfering with the properties of the inner tubes. Also, considering the fluorination process in a nanotube, by performing systematic structural characterizations on heavily fluorinated multiwalled carbon nanotubes, Terrones et al.[12] have revealed that the fluorination process is reversible to some extent, i.e., the F atoms can detach from the carbon network during a heat-treatment process, and this happens without inflicting damage to the carbon network.

Recently, fluorine was also successfully applied as a dopant and a structure modifier in C-based thin films thus achieving a rich variety of structures: fullerene-like, polymeric, and amorphous systems.[13,14] By addressing the effect of the concentration of F incorporated in fullerene-like (FL) carbon fluorides (CF_x), it was found that F concentrations above ∼10 at. % induce amorphyzation of the CF_x film. However, at lower F concentration, of about ∼3−8 at. %, the CF_x films are expected to exhibit more ordered and a moderately cross- and interlocked FL structure. Importantly, in the context of dopants for C-based thin films, F is the strongest performing structure modifier in comparison to N,[15,16] S,[17] and P.[18,19]

A pure and relaxed corannulene molecule (actually, a model system belonging to the class of the polycyclic aromatic hydrocarbons (PAHs) family[20]) possesses a curved-surface geometry representing 1/3 of the cage of a C_{60} fullerene.[21] The corannulene molecule is a widely used model system and a precursor-like species due to its synthesizability[22,23] and its importance as a prototypic building block in organic synthesis,[23,24] as well as for nanounits with expected applications in nanodevices.[25−27]

In contrast to the variety of C-based nanostructured compounds and materials mentioned above, which have been studied both experimentally and theoretically in the context of fluorination, the corannulene molecule (as well as its derivatives) has not been systematically explored as a molecular system capable of yielding structural, energetic, and electronic information for curved 2D C-based materials. This is the aim of

the present study. We have addressed the stability and the electronic properties of F-doped (fluorinated) corannulene molecules in comparison to the hydrogenated ones. In fact, the hydrogenation was employed here as an additional test of our computational approach and comparison with the fluorinated corannulene species since there are a variety of studies by other groups on hydrogenation of coranullene.[28−30]

2. COMPUTATIONAL DETAILS

The calculations for all the systems considered in the present study were carried out by using the Gaussian03 code.[31] We have performed all-electron calculations within density functional theory (DFT), employing the B3LYP[32,33] exchange-correlation functional with the 6-311G(d,p) basis set. This level of theory has been demonstrated to be successful for addressing the structural and electronic properties of similar systems; e.g., in the case of the hydrogenation of corannulene.[28,30]

In total, 36 model systems, containing different F/H concentrations and bonding sites, were fully optimized at the B3LYP/6-311G(d,p) level of theory (see more details in the Supporting Information). In our systematic study, the model system labeled with number one is the pure corannulene molecule (i.e., the benchmark system) while the remaining 35 model systems, result from the substitution of H atoms by different concentrations of F on the edge and/or by doping with F/H atoms the central pentagon of the corannulene molecule. The bowl-shaped corannulene molecule possesses three categories of C atoms, according to their position/bonding: the outermost 10 C bonded to a H atom are labeled as rim C atoms (C_r), the innermost five C atoms on the five-membered ring as hub C atoms (C_h), while the remaining five C atoms, connecting the rim and hub ones are labeled as bridge C atoms (C_b).[34,35]

The calculations were performed in the following sequence. (i) Incorporation of F/H atoms to corannulene's hub C atoms at different sites, also distinguishing between approaching the molecule at its convex or, alternatively, at its concave side, and with different concentrations. (ii) Substitution of an H atom by an F atom at corannulene's rim C atoms. First, we substitute one H by one F atom, then two H atoms by two F atoms, and so on, until all the H atoms at the corannulene edge are substituted by F atoms. (iii) Substitution of an H atom by two F atoms, in order to analyze the effects of the hybridization change of the C atoms at the edge of the corannulene molecule. Also, we have investigated the fully fluorinated system.

To evaluate the structural stability of the model systems investigated here, the cohesive energy per atom ($E_{coh/at}$) is calculated. This is defined as the energy required for breaking the system into the isolated atomic species,[26,36,37] which is given by

$$E_{coh/at} = -(E_{total} - n_C E_C - n_H E_H - n_F E_F)/M \quad (1)$$

where E_{total}, E_C, E_H, and E_F are the total energies of an optimized system, an isolated C atom, an isolated H atom, and an isolated F atom, respectively. The coefficients n_C, n_H, and n_F represent the numbers of carbon, hydrogen, and fluorine atoms belonging to the given model system, respectively. $M = n_C + n_F$ stays for the number of both carbon and fluorine atoms (considered as heavy atoms in comparison to the H atoms). Additionally, the bond energy per added atoms ($E_{bond/at}$), given by

$$E_{bond/at} = -(E_{total} - E_{corannulene} - n E_X)/n \quad (2)$$

was examined in the case of the addition of F/H atoms on the corannulene molecule. In eq 2, $E_{corannulene}$ is the total energy of the isolated molecule, E_X corresponds to the energy of the dopant species, and n is the number of added atoms.

As a reliable criterion for ensuring that the model systems of interest are optimized and represent true energy minima on the potential energy surfaces, their vibrational frequencies were calculated in the harmonic approximation. We report data only for those model systems in which real-valued vibrational frequencies have been obtained.

3. RESULTS AND DISCUSSION

Herein, we report the results for the optimized corannulene molecule and the corresponding systems resulting from it by doping/atomic substitution. Figure 1 displays an identification
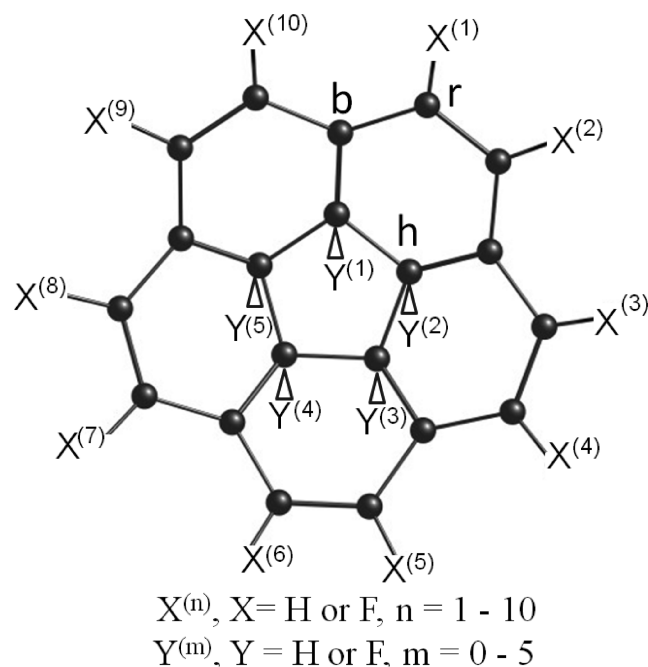

$X^{(n)}$, X = H or F, n = 1 - 10
$Y^{(m)}$, Y = H or F, m = 0 - 5

Figure 1. Identification map introducing the labeling scheme adopted for all the systems studied herein. The indexes "n" and "m" correspond to the number of F and H atoms, while the labels "Y" and "X" correspond to the atomic species and can refer to either the F or H atom. The conformation of the map corresponds to a pure optimized corannulene molecule.

map introducing a general labeling for all systems considered. The indexes "n" and "m" represent the number of F and H atoms, while the labels "Y" and "X" can refer to either the F or H atom. The map topology corresponds to a pure corannulene molecule.

3.1. Fluorination versus Hydrogenation at Corannulene's Hub C Atoms. In total, regarding fluorination and hydrogenation at corannulene's C_h, 25 model systems were optimized being 12 of them hydrogenated and 13 fluorinated. Their stabilities were evaluated by calculating their cohesive energies per atom, beside the frequency analyses. Figure 2 displays the variation of $E_{coh/at}$ with the system (different systems are distinguished by their different number of dopant F and H atoms) for all the hydrogenated and fluorinated model systems at corannulene's C_h. Considering the position or concentration of the H atoms incorporated in the corannulene molecule, $E_{coh/at}$ does not change significantly, being its
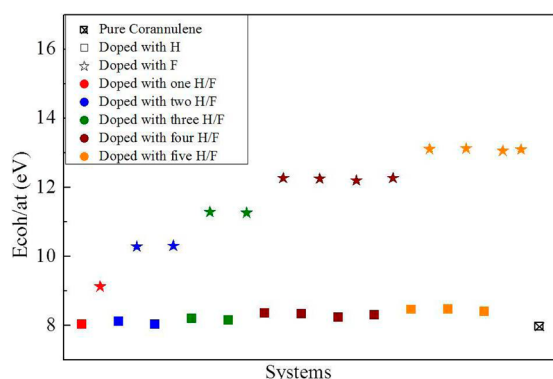
Figure 2. Variation of the cohesive energy per atom ($E_{coh/at}$); a corannulene molecule subjected to hydrogenation and fluorination at its C_h sites. The asterisk corresponds to model systems with F atoms bonded to C_h sites, while the square represents the model systems with H atoms bonded to the C_h sites. The same color marks the system with the same concentration of incorporated F/H at the hub sites.

dispersion for this set of hydrogenated molecules smaller than 0.4 eV.

In contrast, $E_{coh/at}$ considerably increases with the increment of the concentration of F atoms at corannulene's C_h. The energy dispersion corresponding to corannulene's C_h fluorination is ∼4.0 eV. The most stable structures among the molecules obtained by fluorination of corannulene's C_h exhibit peculiar conformations (see Figure 3). Our model systems with the highest cohesive energy per atom are those with five F atoms incorporated (13.13 eV), displayed in Figure 3d. The five F atoms are incorporated at the C_h and distributed as follows: one of the F atoms is incorporated at the concave side, and the four remaining F atoms are bonded at the convex side of the

corannulene molecule. Also, the calculated bond energy per functional group indicates that this structure is the most strongly bound system, giving $E_{bond/at} = 32.93$ eV, whereas the most stable structure containing an even number of F atoms (Figure 3c) reads $E_{bond/at} = 32.90$ eV and a corresponding $E_{coh/at} = 12.27$ eV.

To summarize these results, both the hydrogenation and the fluorination at corannulene's pentagon (i.e., C_h) yield a stabilizing effect on the molecule (cohesive energies varying from 7.97 eV, for the pure corannulene, to an average value of 8.27 eV, when hydrogenation takes place, and to an average value of 11.82 eV, when the corannulene molecule is treated by fluorination). These results clearly indicate that the fluorination compared to hydrogenation at the corannulene's pentagon is by far the most efficient stabilization mechanism when applied to the same topological region (C_h) of the corannulene molecule. These findings can be also confirmed by analyzing the calculated bond energies per added atoms on the corannulene molecule (see values tabulated in the Supporting Information).

3.2. Fluorination at the Bridge C Atoms versus Fluorination at the Hub C Atoms. When the fluorination of the C_b atoms of the corannulene molecule is considered along with the fluorination of corannulene's pentagon (C_h), i.e., when an F atom is being bonded to a C_b position, while another F atom is already attached to a C_h position, the cohesive energies are further increased by an additional value of 0.02 eV, as compared to the case of fluorination at two C_h sites (see Figure 4). In terms of bond energy, this corresponds to a stability of 0.21 eV for the structure displayed in Figure 4b. However, when we consider two F atoms attached onto the same C−C bond in hub C atoms, the most stable structure is the one with both F atoms attached on the convex side of corannulene (see Figure 3a). This situation is also schematically displayed in Figure S27, Supporting Information.
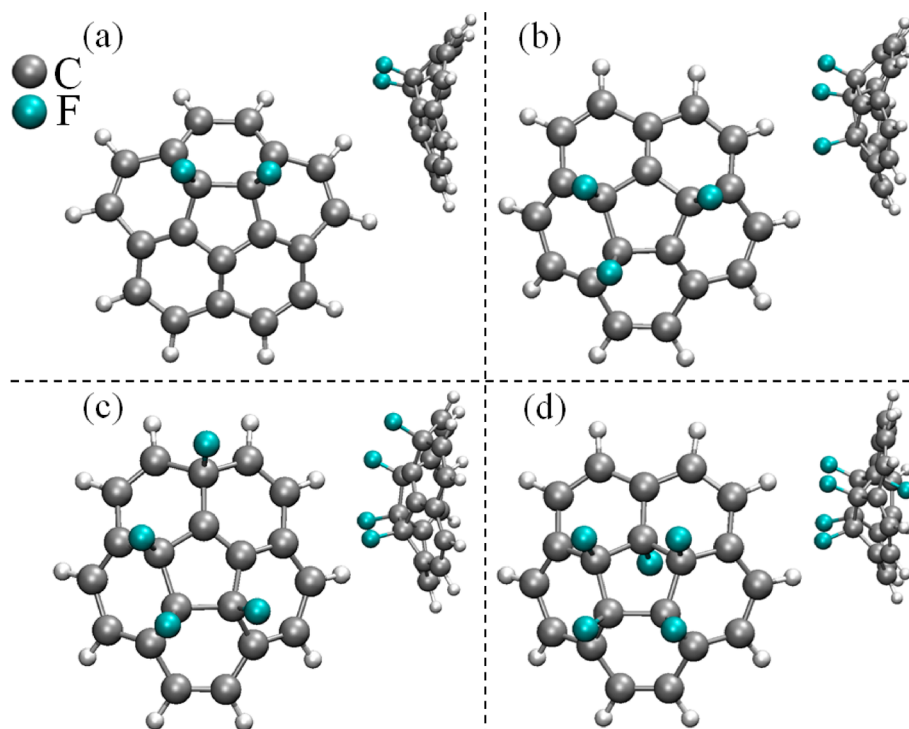

Figure 3. Most stable molecular structure containing two (a), three (b), four (c), and five (d) F atoms incorporated on corannulene's pentagon. The side view of these structures is displayed in the upper right corner of each panel (a)−(d).
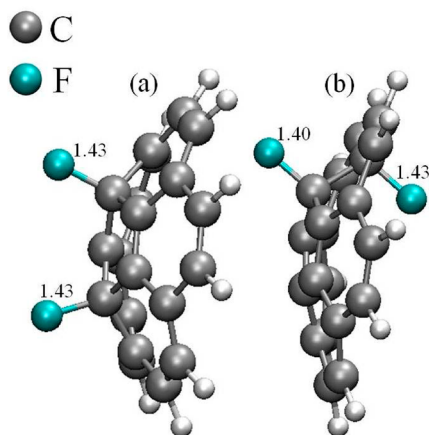
Figure 4. Optimized structures of a corannulene molecule fluorinated by two F atoms: at two C_h sites (a), and at a C_h and a C_b site (b). The latter configuration is energetically more favorable than the structure displayed in panel a. See also Figure S7 in the Supporting Information.

Figure 5. Variation of the cohesive energy per atom ($E_{coh/at}$) as a function of the number of corannulene's peripheral H atom substituted by F atoms.

Except in few cases, it is a general observation, from the results regarding fluorination and hydrogenation at C_h, C_b, and even at the C_r sites (to be discussed in more detail below) of the corannulene molecule, that there is an energetic advantage of both doping processes when they take place on the convex side of the corannulene molecule as opposed to its concave side. When the relaxation procedure starts for a corannulene molecule with one F atom incorporated at its concave side, there happens an inversion of its curvature orientation, after which the F atom persists on the convex side of the optimized system. Our results are in excellent agreement with results on the molecular electrostatic potential of similar systems obtained in other studies.[30,38] These report that the molecular electrostatic potential at the pentagon in the corannulene molecule always exhibit lower negative minima on the convex side than on the concave side.

Considering now some geometric features of these model systems, the average value of the C−F bond lengths obtained for F atoms bonded at a C_b site and at a C_h site is 1.41 Å. Correspondingly, the dispersion of the C−F bond lengths in these cases is only 0.09 Å, with the longest bond length (obtained at a C_b site) being 1.48 Å, while the shortest (obtained at a C_h site) reads 1.39 Å. Note that these C−F bond lengths are similar to those calculated in other theoretical works[8] for similar systems and are also consistent with the corresponding experimental values.

The effects of fluorination at the rim C atoms (C_r) will be discussed in the context of the substitution of H by F atoms.

3.3. Substitution of Corannulene's Peripheral H Atoms by F Atoms. Now, we consider the gradual substitution of corannulene's peripheral H atoms by F atoms. In total, 10 model systems were considered. Figure 5 illustrates the cohesive energy of these model systems as a function of the number of F atoms incorporated. The clear trend obtained in this case is the increment of $E_{coh/at}$ with the number of F atoms incorporated. This behavior indicates that the molecule with all H atoms substituted by F atoms ($C_{20}F_{10}$) is expected to be even more stable than the corannulene molecule ($C_{20}H_{10}$) itself. This prediction is, in general, in agreement with results obtained in studies focused on fluorination of C-based compounds,[39,9] which report that the fluorographene system is 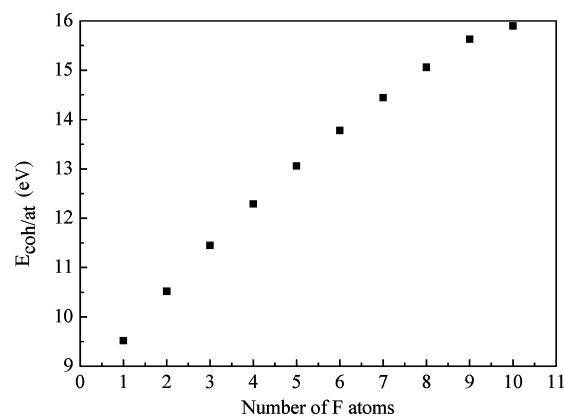more stable than graphane. Fluorographene is a derivative of graphene, a two-dimensional carbon sheet of sp^3 hybridized atoms, where each carbon atom is bound to one F atom.[40] Similarly, graphane is a two-dimensional carbon sheet where each carbon atom is bound to one H atom.[41,8]

The energetic advantage of fluorinated C-based nanostructures and molecules is usually explained by the much higher desorption energy for F_2 as compared to H_2 for a variety of C-based systems. When the first atom in the sequence of 10 H atoms belonging to corannulene's rim C atoms is substituted by an F atom, the cohesive energy increases by 1.55 eV, in comparison to the case of pure corannulene. By replacing the second H atom by an F atom, the stability further increases by another amount of 1.0 eV, and so on. Finally, when the last of the corannulene's H atoms is substituted by an F atom, the cohesive energy increment reads only 0.27 eV. This value still exhibits a considerable gain in structural stability if considered in the context of thermal energies at room temperature (∼0.05 eV) or reaction barriers in organic chemistry synthesis (usually, widely varying between 0.1−1 eV).

The energetic behavior observed for these fluorinated model systems can be extrapolated for larger PAHs and suggests that the cohesive energy curves (i.e., $E_{coh/at}$ as a function of the number of incorporated F atoms) may reach a plateau before all H atoms being substituted by F atoms. This result means that further fluorination after some point would produce only a small energy gain in the system. However, such larger corannulene analogues, in contrast to the corannulene molecule, may not be entirely susceptible to full fluorination. In the case of corannulene, the fully fluorinated molecule is obtained as a stable structure at the present level of calculation. The optimized $C_{20}F_{30}$ structure, exhibiting a cohesive energy of 23.50 eV, is displayed in Figures 6b and S28, Supporting Information. However, in this case, the F atoms bonded to C_b and C_h sites prefer to be alternated in both sides of corannulene. The substitution of all H atoms in corannulene by two F atoms will be discussed further.

It is remarkable that the substitution of the peripheral H atoms of the corannulene molecule by F atoms ensures larger cohesive energy gain than when F (or H) atoms are bonded to the C_h and C_b sites of the corannulene molecule. For example, the bonding of an F atom to corannulene's pentagon (at a C_h site) is associated with a $E_{coh/at}$ gain of 1.16 eV, while the substitution of a peripheral H atom by an F atom brings a gain
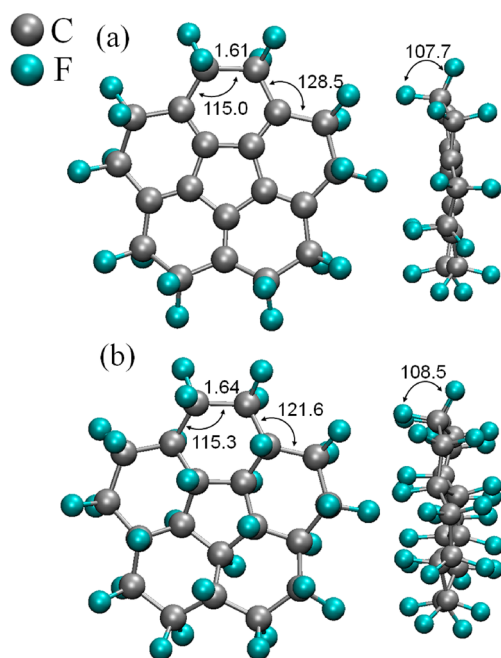
Figure 6. $C_{20}F_{20}$ molecule (a), obtained by substitution of each of the peripheral H atoms of the corannulene molecule by two F atoms, and the fully fluorinated system $C_{20}F_{30}$ (b). The distances are given in angstroms and the angles in degrees.

in $E_{coh/at}$ of 2.41 eV (or 1.25 eV more than the reaction of such a single F atom with corannulene's pentagon).

3.4. Fluorination at Corannulene's Rim C Atoms. The effect of the complete substitution of all H atoms belonging to the corannulene molecule by two F atoms (i.e., bonding two F atoms at each C_r site) is now considered. Figure 6a illustrates the optimized structure of such a corannulene derivative $C_{20}F_{20}$. Also, we have considered this effect in the $C_{20}F_{30}$ molecule (Figures 6b and S28, Supporting Information). Important structural changes observed in the optimized $C_{20}F_{20}$ in comparison to a pure corannulene molecule are summarized in the following:

(i) The C atoms of the entire $C_{20}F_{20}$ lay now almost in the same plane (not the case of the naturally curved corannulene molecule). This phenomenon is due to the change in the hybridization of the C_r atoms from sp^2 hybridization to sp^3 hybridization. Additionally, the rim

carbon atoms C_r tend to acquire tetrahedral coordination thus keeping the bridge carbon atoms C_b in the same plane.

(ii) In the $C_{20}F_{20}$ structure, the average internal angle formed from the C_r atom to the two nearest-neighbor C atoms (which are C_b and C_r sites) is 115° (see Figure 6a), while in pure corannulene, the equivalent angle at 122° is slightly larger. The average external angle $C_r-C_b-C_r$ is 128.5°, while in $C_{20}H_{10}$, it is 129.8°. The average angle involving the two incorporated F atoms, i.e., $F-C_r-F$, is 107.7° in $C_{20}F_{20}$ and 108.4° in $C_{20}F_{30}$. We notice that this may be an interesting feature inherent to the fluorination at the edges of larger polycyclic aromatic hydrocarbons.

(iii) The bond length among the neighboring C_r atoms in $C_{20}F_{20}$ is about 19% longer in comparison to the case of $C_{20}H_{10}$ (in $C_{20}F_{20}$, the average bond length is 1.61 Å in contrast to the value of 1.39 Å in $C_{20}H_{10}$). In order to provide a context for comparison of the bond lengths in our relaxed $C_{20}F_{20}$ system, we also provide here results obtained by others for both the experimental C−C bond lengths in graphite fluoride (1.53 Å)[42] and the theoretically calculated bond lengths in carbon monofluoride (1.55 Å).[43]

The cohesive energy is 20.77 eV for $C_{20}F_{20}$ (and 23.50 eV for $C_{20}F_{30}$), thus confirming that the larger the number of F atoms incorporated in a corannulene molecule, the higher the $E_{coh/at}$. Not surprisingly, this result suggests that $C_{20}F_{20}$ is even more stable than $C_{20}F_{10}$, which in its turn is more stable than the bare corannulene molecule itself. In this direction, we expect that the model systems $C_{20}F_{10}$, $C_{20}F_{20}$, and $C_{20}F_{30}$ should be synthesizable at chemically favorable conditions.

3.5. Electronic Properties and Charge Distribution of Fluorinated and Hydrogenated Corannulene. We shall discuss here the calculated electronic properties of the different fluorinated and hydrogenated corannulene molecules. Table 1 lists the $E_{coh/at}$ gains, the HOMO−LUMO gaps, and the dipole moments together with the dispersions of all these quantities for all the model systems taken into account in this work. The spin multiplicity for all these species is listed in Tables S2−S26 of the Supporting Information. The energy gain $\Delta E_{coh/at}$ is defined here as $\Delta E_{coh/at} = E_{coh/at}$ (fluorinated/hydrogenated system) $- E_{coh/at}$ (isolated corannulene). The dispersion value provided for each quantity equals the average value of this quantity minus the largest (or smallest) value of the same

Table 1. Gains in Cohesive Energy Per Atom ($\Delta E_{coh/at}$), HOMO−LUMO Gaps (E_g), and Dipole Moments (μ) Calculated for the Fluorinated and Hydrogenated Corannulene Molecules; Labels Are in Accordance to Those Introduced in Figure 1

	H (incorporated)			F (incorporated)			F (substituted)		
concentration	$\Delta E_{coh/at}$ (eV)	E_g (eV)	μ (D)	$\Delta E_{coh/at}$ (eV)	E_g (eV)	μ (D)	$\Delta E_{coh/at}$ (eV)	E_g (eV)	μ (D)
1	0.07	0.53	1.55	1.16	0.71	0.39	1.55	2.95	2.41
2	0.11 ± 0.04	0.72 ± 0.18	1.49 ± 0.02	2.33 ± 0.01	1.74 ± 0.69	3.67 ± 1.81	2.55	2.83	3.24
3	0.22 ± 0.03	0.60 ± 0.02	0.85 ± 0.28	3.31 ± 0.02	0.27 ± 0.14	4.87 ± 1.46	3.48	2.83	4.16
4	0.35 ± 0.07	1.36 ± 0.28	0.90 ± 0.22	4.28 ± 0.05	1.54 ± 0.06	5.26 ± 1.99	4.32	2.85	4.69
5	0.48 ± 0.04	0.39 ± 0.01	0.58 ± 0.36	5.13 ± 0.04	0.46 ± 0.06	5.21 ± 2.80	5.09	2.88	4.90
6							5.81	2.78	4.58
7							6.47	2.74	3.91
8							7.09	2.72	2.88
9							7.66	2.75	1.77
10							7.93	2.79	1.36
20	1.73	0.38					12.80	3.46	0.69

quantity. For those quantities for which only one value is calculated (or a single geometric conformation is optimized), the dispersion is zero.

As expected for doped C-based nanostructures, we have obtained that the hydrogenation or fluorination significantly changes the HOMO−LUMO gap of the corannulene molecule (see Table 1). As a reference, the calculated HOMO−LUMO gap for the pristine corannulene molecule is 3.08 eV, which agrees very well with theoretical results by others obtained at the same level of theory.[44] Indeed, the energy gap has been considered as a measure of kinetic stability of distinct doped systems.[44] However, for these F/H-doped systems, a simple relationship between HOMO−LUMO gaps and cohesive energies is not observed. With the exception of the $C_{20}F_{20}$ for which we obtain a HOMO−LUMO gap of 3.46 eV (i.e., $C_{20}F_{20}$ possesses a gap that is 12.3% larger than that of an isolated corannulene molecule), most of the other fluorinated and hydrogenated model systems exhibit smaller HOMO−LUMO gaps than that of bare corannulene (see Table 1).

The optimized systems with an odd number of F atoms incorporated are doublet, while the ones with an even number of F atoms incorporated are singlet. As a consequence, the systems with an odd number of F atoms possess smaller HOMO−LUMO gaps than those systems with an even number of F atoms (see Table 1). Considering the monofluorinated system, we point out that its cohesive energy of 9.13 eV is associated with the HOMO−LUMO gap of 0.71 eV. For the trifluorinated systems, the most stable structure, with cohesive energy of 11.29 eV, exhibits a HOMO−LUMO gap of 0.13 eV, while the less stable system, with cohesive energy of 11.26 eV, exhibits a gap of 0.41 eV. In the case of the most stable penta-fluorinated system, with a cohesive energy of 13.11 eV, the HOMO−LUMO gap is 0.45 eV.

Considering now the spin-singlet fluorinated systems, the less stable difluorinated structure, with a cohesive energy of 10.29 eV, exhibits a gap of 1.05 eV; whereas the most stable structure, with a cohesive energy of 10.31 eV, exhibits a very large gap of 2.42 eV. This relationship is not, however, kept valid for the tetra-fluorinated structures. For example, the most stable structure ($E_{coh/at}$ = 12.27 eV) has a gap of 1.53 eV, the structure with $E_{coh/at}$ = 12.25 eV has a gap of 1.48 eV, and the less stable structure ($E_{coh/at}$ = 12.20 eV) has a gap of 1.56 eV. Thus, these results are not directly in line with the general observation that a large HOMO−LUMO gap is often associated with high kinetic stability.

It is also worth mentioning that, when 20 H atoms are incorporated at corannulene's periphery, the calculated HOMO−LUMO gap is 0.38 eV, which is a very significant decrease in comparison to the pure corannulene (HOMO−LUMO gap = 3.08 eV). In contrast, when all H atoms of a corannulene molecule are substituted by 20 F atoms, the calculated HOMO−LUMO gap is 3.46 eV, a value which is higher than the HOMO−LUMO gap of the pure corannulene molecule.

Before discussing the charge distribution in these model systems, we have analyzed their electric dipole moments. As seen from the values listed in Table 1, the dipole moment of a doped system strongly depends of the positions and the concentration of F/H bonded or substituted in the corannulene molecule. For example, in the case of five F atoms bonded to the convex side of the corannulene molecule, the dipole moment reads μ = 7.34 D, while the dipole moment decreases to μ = 2.41 D, when three F of these five F atoms are bonded at

the convex side of the corannulene molecule, and the remaining two F atoms are bonded at its concave side. For comparison, the dipole moment of a bare corannulene molecule is 2.03 D. As noticed for these systems, there is no systematic behavior for the dipole moment as a function of the number of dopant atoms.

In the Supporting Information, the frontier molecular orbitals of all the model systems studied here are plotted in Figures S39−S90. As can be seen from the HOMO plots, when two or more F atoms are bonded to corannulene's pentagon, the charge distribution is more localized in the region of the C_r and C_b (in contrast to the pure corannulene molecule, where the largest charge distribution belongs to the region of the C_h). When the degree of fluorination of the corannulene molecule increases, more and more pronounced concentration of charge on the edge carbon atoms (mostly at the C_r's but also at the C_b's) is obtained.

Using the Bader charge analysis method,[45] we have evaluated the charge transfer (CT) between the corannulene molecule and the F atoms. These results are presented in Table 2. Not

Table 2. Average Charge Transfer (CT) for the Fluorinated Corannulene Molecule Obtained by using Bader's Analysis; in All Cases the Resulting CT Occurs from the C Atoms to the F Atoms

model system	average charge transfer (e)
1 F atom incorporated	+0.60
1 F atom substituted	+0.76
2 F atom incorporated	+0.70
2 F atom substituted	+0.77
10 F atoms substituted	+0.77
20 F atoms substituted	+0.82

surprisingly, in all cases, there is a charge transfer from the carbon atoms to the F atoms. In general, the higher the number of F atoms incorporated into the corannulene molecule, the higher the CT to each one of the F atoms. We have also noticed that the CT in the structures with H atoms substituted by F atoms is higher than the CT in the structures with F atoms incorporated. For example, in a system in which an H atom is substituted by an F atom, the charge transfer is +0.76e (the plus sign meaning that the F atom gains charge from the carbon atoms), while in the case of one F atom incorporated in corannulene's pentagon, the charge transfer reads +0.60e.

■ CONCLUSIONS

We have carried out a systematic DFT study of the structural and electronic properties of H-doped (hydrogenated) and F-doped (fluorinated) corannulene molecule, which is a prototype of a curved 2D carbon structure. We have examined the impact of the incorporation of F/H atoms at different concentrations and sites in corannulene and also the substitution of each peripheral H atom of the corannulene molecule by one or two F atoms. Our results demonstrate that the fluorinated corannulene systems are considerably more stable than their hydrogenated analogues. Both the $C_{20}F_{10}$ (in which all peripheral H atoms are substituted by F atoms) and the $C_{20}F_{20}$ (in which all peripheral H atoms are substituted by two F atoms) are more stable than the bare corannulene molecule. In fact, the $C_{20}F_{20}$ ($E_{coh/at}$ = 20.77 eV) is even more stable than $C_{20}F_{10}$ ($E_{coh/at}$ = 15.90 eV), which in turn is more stable than the bare corannulene molecule itself ($E_{coh/at}$ = 7.97

eV), thus suggesting that both $C_{20}F_{20}$ and $C_{20}F_{10}$ may be synthesizable at favorable chemical conditions.

However, the gain in cohesive energy corresponding to the substitution of two peripheral H atoms in a corannulene molecule by two F atoms ($\Delta E_{\text{coh/at}}$ = 2.55 eV) is larger than the gain in cohesive energy ($\Delta E_{\text{coh/at}}$ = 1.73 eV) when a whole sequence of 10 additional H atoms are bonded to the corannulene molecule giving $C_{20}H_{20}$. In a topological context, the F atoms bonded to the C_r sites of the corannulene molecule bring a larger gain in cohesive energy than those F atoms bonded to the C_h sites. Furthermore, the cohesive energies of the systems considered in this work do not exhibit a simple relationship with their HOMO−LUMO gaps, as expected for related doped systems. Indeed, the variation of the HOMO−LUMO gap strongly depends on the concentration and the position of the incorporated F atoms.

The stability of the fluorinated corannulene systems and their tunable properties, obtained by controlling the degree of fluorination, which we have systematized and discussed in this article, is of interest for potential applications of larger curved 2D carbon nanostructures. Also, the prototypical role of the small PAHs in organic synthesis and as possible building blocks for nanotemplates applicable for building nanodevices is expected to encourage experiments focused on corannulene fluorination, as well as separation, and purification of fluorinated corannulene molecules. In the context of fluorination, this study may support attempts for experimental works on the electronic and charge transfer properties of C-based nanostructures.

■ ASSOCIATED CONTENT

Ⓢ Supporting Information

Optimized structures, spin multiplicities, bond and cohesive energies, and frontiers molecular orbitals. This material is available free of charge via the Internet at http://pubs.acs.org.

■ AUTHOR INFORMATION

Corresponding Author

*E-mail: renatobs@ufba.br (R.B.d.S.); rivelino@ufba.br (R.R.); fbmota@ufba.br (F.d.B.M.); gekos@ifm.liu.se (G.K.G).

Notes

The authors declare no competing financial interest.

■ ACKNOWLEDGMENTS

■ REFERENCES

(1) Touhara, H.; Okino, F. *Carbon* **2000**, *38*, 241−267.
(2) Cheng, S.-H.; Zou, K.; Okino, F.; Gutierrez, H. R.; Gupta, A.; Shen, N.; Eklund, P. C.; Sofo, J. O.; Zhu, J. *Phys. Rev. B* **2010**, *81*, 205435.
(3) Touhara, H.; Inahara, J.; Mizuno, T.; Yokoyama, Y.; Okanao, S.; Yanagiuch, K.; Mukopadhyay, I.; Kawasakia, S.; Okino, F.; Shirai, H.; Xu, W. H.; Kyotani, T.; Tomita, A. *J. Fluorine Chem.* **2002**, *114*, 181−188.
(4) Lee, Y.-S. *J. Fluorine Chem.* **2007**, *128*, 392−403.
(5) Hayashi, T.; Shimamoto, D.; Kim, Y. A.; Muramatsu, H.; Okino, F.; Touhara, H. *ACS Nano* **2008**, *2*, 485−488.
(6) Boukhvalov, D. W.; Katsnelson, M. I. *J. Phys.: Condens. Matter* **2009**, *21*, 344205.
(7) Nair, R. R.; Ren, W.; Jalil, R.; Riaz, I.; Kravets, V. G.; Britnell, L.; Blake, P. *Small* **2010**, *6*, 2877−2884.
(8) Medeiros, P. V. C.; Mascarenhas, A. J. S.; Mota, F. B.; Castilho, C. M. C. *Nanotechnology* **2010**, *21*, 485701.
(9) Zboril, R.; Karlicky, F.; Bourlinos, A. B.; Steriotis, T. A.; Stubos, A. K. *Small* **2010**, *6*, 2885−2891.
(10) Samarakoon, D. K.; Chen, Z.; Nicolas, C.; Wang, X. Q. *Small* **2011**, *7*, 965−969.
(11) Sahin, H.; Topsakal, M.; Ciraci, S. *Phys. Rev. B* **2011**, *83*, 115432.
(12) Hayashi, T.; Terrones, M.; Scheu, C.; Kim, Y. A.; Ru1hle, M.; Nakajima, T.; Endo, M. *Nano Lett.* **2002**, *2*, 491−496.
(13) Schmidt, S.; Greczynski, G.; Goyenola, C.; Gueorguiev, G. K.; Czigány, Z.; Jensen, J.; Ivanov, I. G.; Hultman, L. *Surf. Coat. Technol.* **2011**, *206*, 646−653.
(14) Gueorguiev, G. K.; Goyenola, C.; Schmidt, S.; Hultman, L. *Chem. Phys. Lett.* **2011**, *516*, 62−67.
(15) Gueorguiev, G. K.; Neidhardt, J.; Stafström, S.; Hultman, L. *Chem. Phys. Lett.* **2008**, *410*, 228−234.
(16) Broitman, E.; Gueorguiev, G. K.; Furlan, A.; Son, N. T.; Gellman, A. J.; Stafström, S.; Hultman, L. *Thin Solid Films* **2008**, *517*, 1106−1110.
(17) Goyenola, C.; Gueorguiev, G. K.; Stafström, S.; Hultman, L. *Chem. Phys. Lett.* **2011**, *506*, 86−91.
(18) Furlan, A.; Gueorguiev, G. K.; Czigány, Z.; Högberg, H.; Braun, S.; Stafström, S.; Hultman, L. *Phys. Status Solidi RRL* **2008**, *2*, 191−193.
(19) Furlan, A.; Gueorguiev, G. K.; Högberg, H.; Stafström, S.; Hultman, L. *Thin Solid Films* **2006**, *515*, 1028−1032.
(20) Tielens, A. G. G. M. *Annu. Rev. Astron. Astrophys.* **2008**, *46*, 289−337.
(21) Denift, S.; Sonnweber, B.; Mack, J.; Scott, L. T.; Scheier, P.; Becker, K.; Märk, T. D. *Int. J. Mass Spectrom.* **2006**, *249−250*, 353−358.
(22) Barth, W. E.; Lawton, R. G. *J. Am. Chem. Soc.* **1971**, *93*, 1730−1745.
(23) Seiders, T. J.; Elliott, E. L.; Grube, G. H.; Siegel, J. S. *J. Am. Chem. Soc.* **1999**, *121*, 7804−7813.
(24) Steinberg, B. D.; Jackson, E. A.; Filatov, A. S.; Wakamiya, A.; Petrukhina, M. A.; Scott, L. T. *J. Am. Chem. Soc.* **2009**, *131*, 10537−10545.
(25) Rivelino, R.; Santos, R. B.; Mota, F. B.; Gueorguiev, G. K. *J. Phys. Chem. C* **2010**, *114*, 16367−16372.
(26) Santos, R. B.; Rivelino, R.; Mota, F. B.; Gueorguiev, G. K. *Phys. Rev. B* **2011**, *84*, 075417.
(27) Bauert, T.; Merz, L.; Bandera, D.; Parschau, M.; Siegel, J. S.; Ernst, K.-H. *J. Am. Chem. Soc.* **2009**, *131*, 3460−3461.
(28) Galué, H. A.; Rice, C. A.; Steill, J. D.; Oomens, J. *J. Chem. Phys.* **2011**, *134*, 054310.
(29) Galué, H. A.; Oomens, J. *Astrophys. J.* **2012**, *746*, 83.
(30) Frash, M. V.; Hopkinson, A. C.; Bohme, D. K. *J. Am. Chem.Soc.* **2001**, *123*, 6687−6695.
(31) Frisch, M. J.; et al. *Gaussian 03*, revision D.01; Gaussian Inc.: Wallingford CT, 2004.
(32) Becke, A. D. *J. Chem. Phys.* **1993**, *98*, 5648−5652.
(33) Lee, C.; Yang, W.; Parr, R. G. *Phys. Rev. B* **1988**, *37*, 785−789.
(34) Dobrowolski, M. A.; Ciesielski, A.; Cyranski, M. K. *Phys. Chem. Chem. Phys.* **2011**, *13*, 20557−20563.
(35) Josa, D.; Otero, J. R.; Lago, E. M. C. *Chem. Phys.* **2011**, *13*, 21139−21145.
(36) Gueorguiev, G. K.; Neidhardt, J.; Stafström, S.; Hultman, L. *Chem. Phys. Lett.* **2005**, *401*, 288−295.

(37) Gueorguiev, G. K.; Pacheco, J. M.; Stafström, S.; Hultman, L. *Thin Solid Films* **2006**, *515*, 1192−1196.

(38) Carrazana-Gracía, J. A.; Rodrígues-Otero, J.; Cabeiro-Lago, E. M. *J. Phys. Chem. B* **2011**, *115*, 2774−2782.

(39) Leenaerts, O.; Peelaers, H.; Hernández-Nieves, A. D.; Partoens, B.; Peeters, F. M. *Phys. Rev. B* **2010**, *82*, 195436.

(40) Markevich, A.; Jones, R.; Briddon, P. R. *Phys. Rev. B* **2011**, *84*, 115439.

(41) Sofo, J. O.; Chaudhari, A. S.; Barber, G. D. *Phys. Rev. B* **2007**, *75*, 153401.

(42) Touhara, H.; Kadono, K.; Fujii, Y.; Watanabe, N. *Z. Anorg. Allg. Chem.* **1987**, *544*, 7−20.

(43) Artyukhov, V. I.; Chernozatonskii, L. A. *J. Phys. Chem. A* **2010**, *114*, 5389−5396.

(44) Denis, P. A. *J. Mol. Struct.* **2008**, *865*, 8−13.

(45) Tang, W.; Sanville, E.; Henkelman, G. *J. Phys.: Condens. Matter* **2009**, *21*, 084204.